

Criticality in Alternating Layered Ising Models :

I. Effects of connectivity and proximity

Helen Au-Yang

*Department of Physics, Oklahoma State University,
145 Physical Sciences, Stillwater, OK 74078-3072, USA**

Michael E Fisher

*Institute for Physical Science and Technology,
University of Maryland, College Park, MD 20742-8510†*

The specific heats of exactly solvable alternating layered planar Ising models with strips of width m_1 lattice spacings and “strong” couplings J_1 sandwiched between strips of width m_2 and “weak” coupling J_2 , have been studied numerically to investigate the effects of connectivity and proximity. We find that the enhancements of the specific heats of the strong layers and of the overall or ‘bulk’ critical temperature, $T_c(J_1, J_2; m_1, m_2)$, arising from the collective effects reflect the observations of Gasparini and coworkers in experiments on confined superfluid helium. Explicitly, we demonstrate that finite-size scaling holds in the vicinity of the upper limiting critical point $T_{1c} (\propto J_1/k_B)$ and close to the corresponding lower critical limit $T_{2c} (\propto J_2/k_B)$ when m_1 and m_2 increase. However, the residual *enhancement*, defined via appropriate subtractions of leading contributions from the total specific heat, is dominated (away from T_{1c}) by a decay factor $1/(m_1 + m_2)$ arising from the *seams* (or boundaries) separating the strips; close to T_{1c} the decay is slower by a factor $\ln(m_1/m_0)$.

I. INTRODUCTION

Many experiments performed on ^4He at the superfluid transition in various spatial dimensions¹, reveal excellent agreement with general finite-size scaling theory^{2,3}. Furthermore, when small boxes or “quantum dots” of helium were coupled through a thin helium film, the effects of connectivity and proximity were discovered and quantified⁴⁻⁸.

To gain some more detailed theoretical insights into the proximity effects, we study here the specific heats of an alternating layered planar Ising model, which consists of infinite strips of width m_1 lattice spacings in which the coupling energy between the nearest-neighbor Ising spins is J_1 , separated by other infinite strips of width m_2 whose coupling J_2 is weaker. This is illustrated in Fig.1.

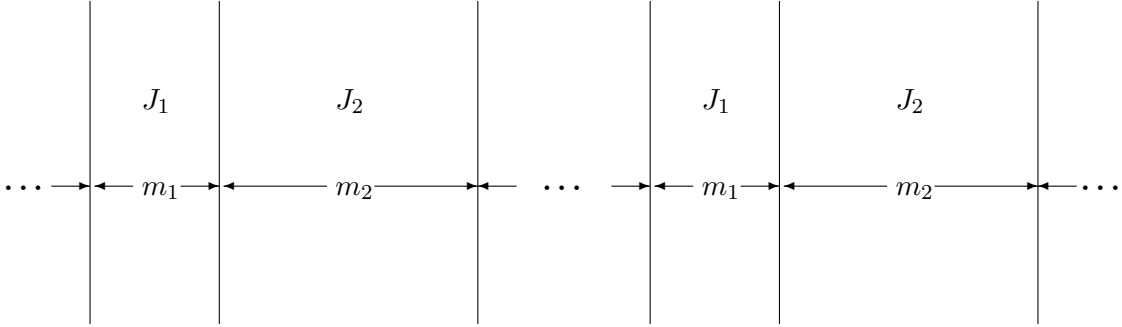


FIG. 1. The planar, square lattice alternating layered Ising model considered. The widths m_1 and m_2 are measured in nearest neighbor lattice spacings while nearest-neighbor Ising spins $\sigma_i = \pm 1$ are coupled via pair Hamiltonians $J_{ij}\sigma_i\sigma_j$.

When J_2 vanishes, the model becomes a system of noninteracting infinite strips of finite width, each of which essentially behaves as a one dimensional Ising model.

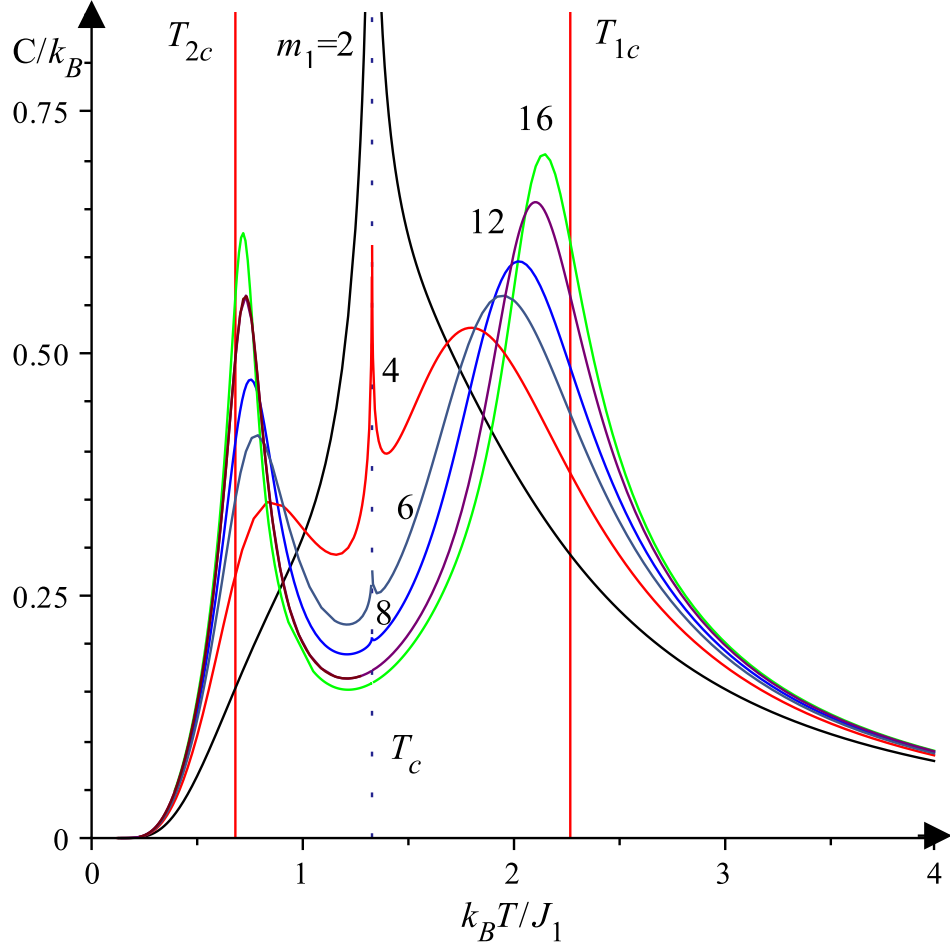


FIG. 2. (a) The specific heats per site of layered systems with relative strength $r = J_2/J_1 = 0.3$ and relative separation $s = 1$ for $m_1 = m_2 = 2, 4, 6, 8, 12$ and 16 . The amplitude $A(r, s)$ of the logarithmic divergence at $T_c(r, s)$, which dominates for $m_1 = 2$, decreases rapidly as m_1 increases. Thus, the small spike at the “true” bulk critical point, T_c , becomes barely visible for $m_1 \geq 8$. However, as demonstrated in Fig. 2(b), it remains evident at larger values of m_1 when r increases towards unity. On the other hand as $A(r, s)$ becomes small two quite distinct rounded peaks appear and move toward the limiting values T_{1c} and T_{2c} as $m_1 = m_2 \rightarrow \infty$.

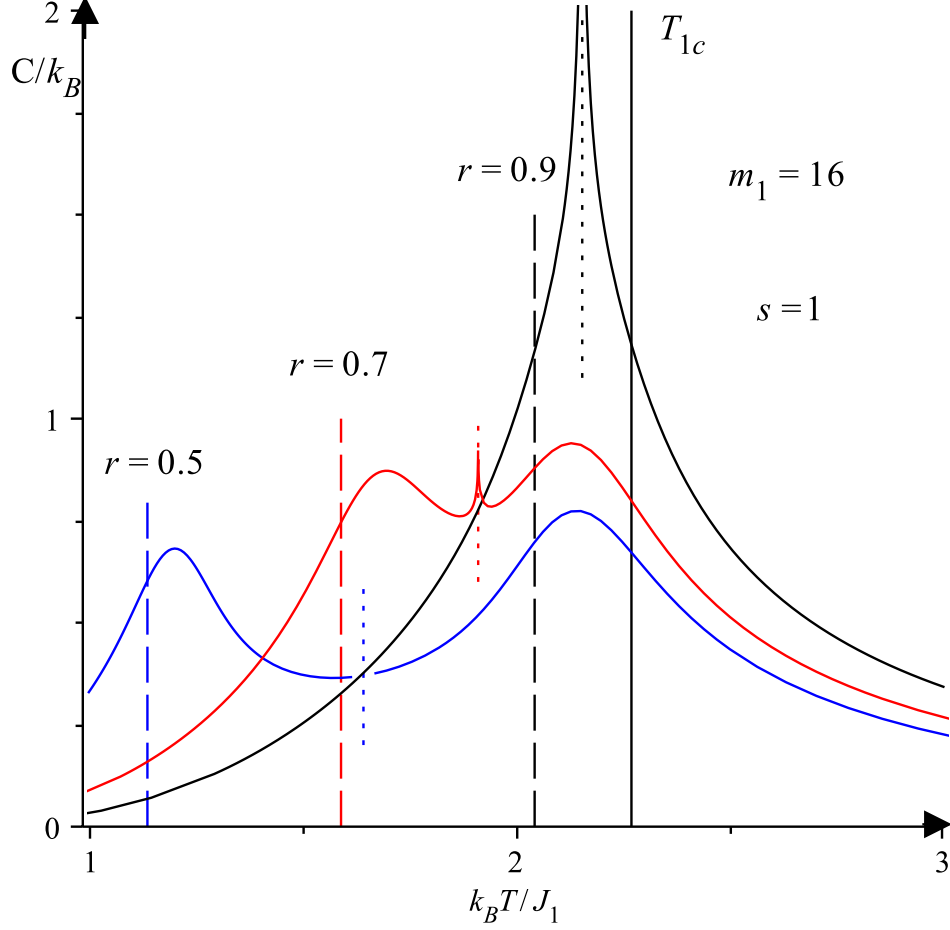


FIG. 2. (b) Plots of the specific heats for fixed $m_1 = m_2 = 16$ and so $s = 1$ but for increasing relative strength r . Note that the logarithmic peak at the overall or bulk critical point, $T_c(r, s)$, indicated by short vertical dotted lines, remains clearly visible when $r = 0.7$ and still dominates entirely when $r = 0.9$.

This means, in particular, that the specific heat is not divergent but rather has a fully analytic rounded peak. However, as long as $J_2 \neq 0$, the system is a two-dimensional bulk Ising model, whose specific heat per site diverges logarithmically at a unique

bulk critical temperature $T_c(J_1, J_2; m_1, m_2)$ in the form

$$C(T)/k_B \propto -A(r, s) \ln |1 - T/T_c| + \cdots, \quad (1)$$

where we have introduced the basic weakness or coupling ratio, r , and the relative separation distance, s , namely

$$r = J_2/J_1 < 1, \quad s = m_2/m_1. \quad (2)$$

In fact, as will be shown⁹, the amplitude $A(r, s)$ of the logarithmic divergence decays exponentially as a function of the minimum of m_1 and m_2 ; indeed, at fixed s and $r \rightarrow 1$, the amplitude decays as $Qm_1e^{-Qm_1}$, where $Q \propto (1 - r)s/(1 + s)$ as $m_1 \rightarrow \infty$. This behavior is evident for $r = 0.3$ in Fig. 2(a), which shows that the divergence, while obvious and dominant for $m_1 = m_2 < 3$, rapidly becomes no more than a minuscule spike, which soon becomes invisible on any graphical plot. On the other hand, for greater values of the coupling ratio r the logarithmic divergence remains dominant for larger values of m_1 and m_2 as seen in Fig. 2(b). But returning to Fig. 2(a) with $r = 0.3$, one observes that as soon as the strip widths, $m_1 = m_2$, exceed three lattice spacings, there appear two further specific heat peaks, albeit rounded; these grow rapidly in height and sharpness and as m_1 and m_2 grow in magnitude, they soon dominate the plots.

Now Fig. 2 is based on exact analytic calculations expounded in Part II of this article⁹. In fact, the analysis of the finite-size behavior of planar Ising models based on the exact solution of Onsager, as extended by Kaufman¹⁰, goes back to the work of Fisher and Ferdinand^{11,12} in 1969. Specifically, the solubility of arbitrarily layered planar Ising models was first noted and reported at a conference in Japan¹², while, independently, McCoy and Wu¹³ developed and analyzed *randomly* layered Ising models. The thermodynamics for regularly layered models was developed by Au-Yang and McCoy¹⁴ and Hamm¹⁵, while the scaling behavior of a single strip of finite width was elucidated by Au-Yang and Fisher¹⁶.

In general the bulk critical temperature can be simply stated, for a layered distribution as¹²

$$k_B T_c \langle\langle \ln \coth(J_x/k_B T_c) \rangle\rangle = 2 \langle\langle J_y \rangle\rangle, \quad (3)$$

where the brackets $\langle\langle \cdot \rangle\rangle$ denote an average over the distribution, random or regular of the distinct number (say $n < \infty$) of lattice spacings constituting a layer of finite width. For the alternating layered Ising model, this becomes

$$2J_1(1 + rs) = k_B T_c [\ln \coth(J_1/k_B T_c) + s \ln \coth(rJ_1/k_B T_c)], \quad (4)$$

which depends only on the weakness ratio r and the relative separation s .

Then as m_1 and m_2 become large, the upper and lower rounded peaks approach limiting values, T_{1c} and T_{2c} (as evident in Fig. 2(a)), which, in fact, match the corresponding bulk (i.e., uniform) two-dimensional Ising models with coupling constants J_1 and J_2 . Thus the limiting values T_{1c} and $T_{2c}(r)$ are known^{10,11,13} and given by

$$k_B T_{1c}/J_1 \simeq 2.269185312, \quad k_B T_{2c}/J_1 \simeq r \cdot 2.269185312. \quad (5)$$

It proves easy to establish the expected inequalities

$$T_{2c}(r) \leq T_c(r, s) \leq T_{1c}. \quad (6)$$

II. QUALITATIVE OBSERVATIONS

To explore further and develop the analogies with the observations on superfluid helium systems, we retain the value of the weakness ratio $r = 0.3$ (used in Fig. 2(a)) but increase the relative layer separation to $s = 2$. The results for $m_1 = 8$ and 16 (as used in Fig. 2(a)) are presented in Fig. 3: see the solid curves. As anticipated, no sign of any singularity at T_c is visible. It should be noted, nonetheless, that were one to examine the overall *spontaneous magnetization*, $M_0(T)$, one would find — and

on a plot “see” — that M_0 vanished identically for $T > T_c$ but was nonzero (and varying as $\propto (T_c - T)^\beta$ with $\beta = \frac{1}{8}$ for 2D Ising layers^{2,3,13}) as soon as $T < T_c$. In the experiments on superfluids the analogous statement concerns the overall *superfluid density* $\rho_s(T)$ ¹; this vanishes identically above the overall or bulk lambda transition at $T_\lambda (\equiv T_c)$ but is detectable, via setting up persistent superflow fluid currents, below T_λ ^{5,7}. (In a bulk 3D superfluid $\rho_s(T)$ varies as $(T_\lambda - T)^\zeta$ with $\zeta \simeq 0.67$, but in a planar 2D superfluid, $\rho_s(T)$ increases discontinuously at the corresponding lambda point, T_λ , on lowering the temperature¹.)

On the other hand, the temperatures of the upper and lower rounded maxima increase (and decrease, respectively), as m_1 increases in Fig. 3. But now, using the explicit results for the infinite strip of finite width¹⁶, we also show, as dashed curves in Fig. 3, the totally decoupled $r = 0$ (or $J_2 = 0$) plots for the two cases $m_1 = 8$ and 16. Clearly the uncoupled upper maxima fall below T_{1c} just as do the coupled ($r = 0.3$) results. (It is worth remarking, however, that for a finite $n \times n$ Ising lattice with *periodic* boundary conditions, as studied by Ferdinand and Fisher¹¹, the maxima in the specific heats lie *above* the bulk critical temperature T_{1c} .) Nevertheless, there is clear evidence of a *coupling* or *proximity* effect in that the specific heats for the alternating, coupled system lie markedly *above* those for the decoupled ($r = 0$) strips. This same effect is seen in the experiments when finite boxes are coupled by a helium film^{5,7}.

Complementary phenomena are observed around the lower maxima. Thus the dotted plots in Fig. 3 show the finite-width result for the situation $r \rightarrow \infty$, or, more intuitively, $J_1 = 0$, for $m_1 = 8$ and 16 (i.e., $m_2 = 16$ and 32). These decoupled specific heats appear as very sharp, but still finitely rounded, spikes. However, it must be noted that these $r \rightarrow \infty$ maxima lie *below* T_{2c} , in accord with expectation for a finite-width strip. On the other hand, the maxima of the coupled alternating system lie *above* the limiting value T_{2c} as seen clearly in the inset in Fig. 3. Once

again there is an unmistakable proximity or enhancement effect that is found also in the experimental studies^{5,7}.

As a next step of our qualitative exploration, we present in Fig. 4 the effects of varying the relative separation s for significantly wide, $m_1 = 18$, strips spaced apart by weaker strips of relative strength $r = 0.3$ (as before). In this case the first point to notice is that $T_c(r, s)$ increases quite rapidly towards T_{1c} as the separation s approaches zero. Next, the uncoupled ($r = 0$) specific heats near T_{1c} (shown dashed as in Fig. 3) all have maxima located at the same temperature, determined only by $m_1 = 18$ for a finite width strips, while their magnitude is determined by s simply via normalization, either through relative area or on a per-site basis. However, there is still clear enhancement in the coupled layers even though the corresponding rounded maxima deviate very little in location from the uncoupled case. By contrast near T_{2c} , as illustrated by the inset, the displacements even of the uncoupled maxima (shown dotted), depend significantly on the relative separation ratio s . Again, nonetheless, there is proximity induced enhancement of the peaks both in magnitude and displacement above T_{2c} .

Finally, we may enquire about the level of the specific heats around the bulk critical point T_c or in the vicinity of the minima observed in Figs. 2-4 that lie roughly at $T_{min} \lesssim \frac{1}{2}(T_{1c} + T_{2c})$. One may ask, for example, how well the levels are approximated by appropriately weighted sums of the uncoupled peaks around T_{1c} plus some, perhaps reversed contribution from T_{2c} . For these purposes, however, we need to proceed more quantitatively.

III. SCALING EXPLORATIONS

We would like to relate the observations embodied in Figs. 2-4 to more general scaling concepts. To this end, recall^{2,3,11,12} that a bulk system with a critical tem-

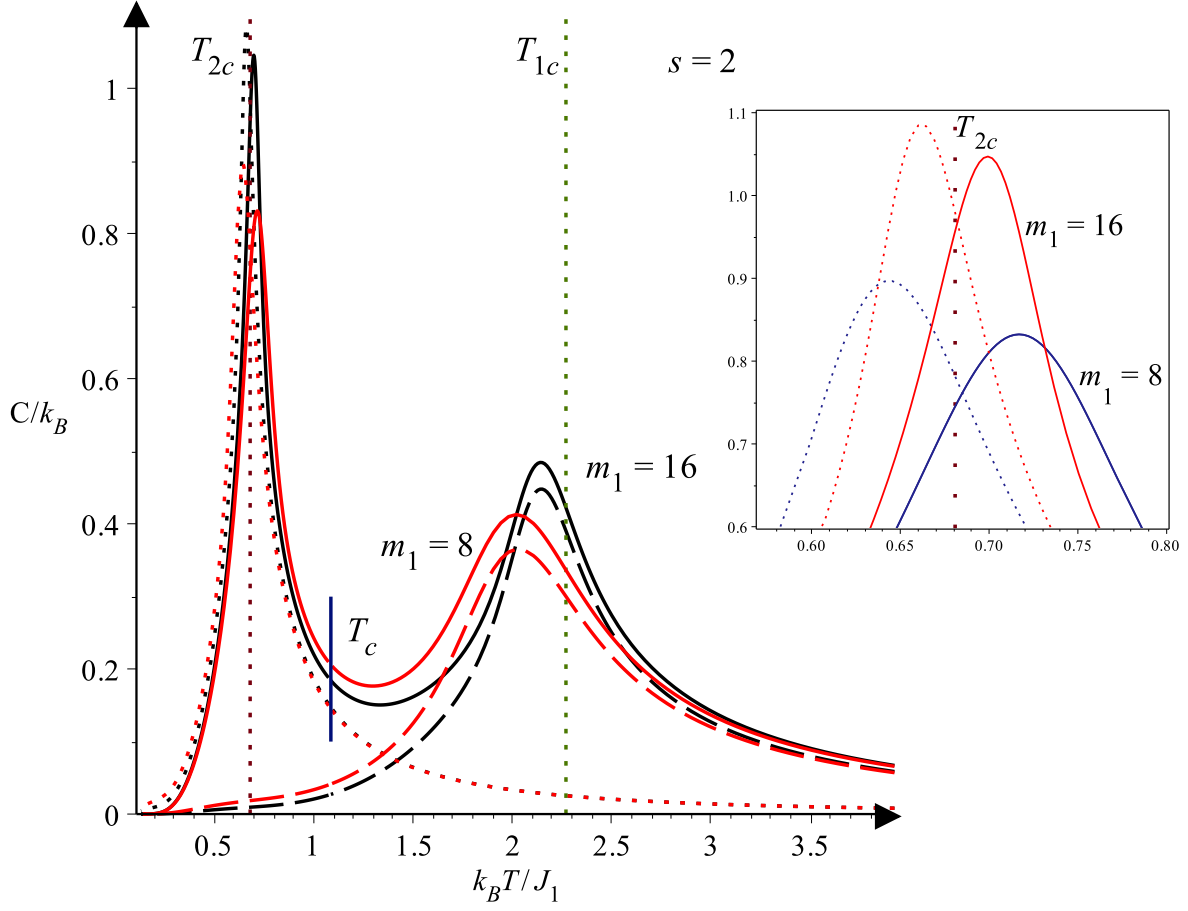


FIG. 3. The specific heats of alternating layered Ising models with relative strength $r = 0.3$ (as in Fig.2(a)) and relative separation $s = 2$ for $m_1 = 8, 16$. The dashed plots denote the corresponding decoupled specific heats when $J_2 = 0$ ($r = 0$), while the dotted lines represent the specific heats when $J_1 = 0$ (or $r \rightarrow \infty$). The inset displays the distinct maxima near T_{2c} , dotted below but solid above.

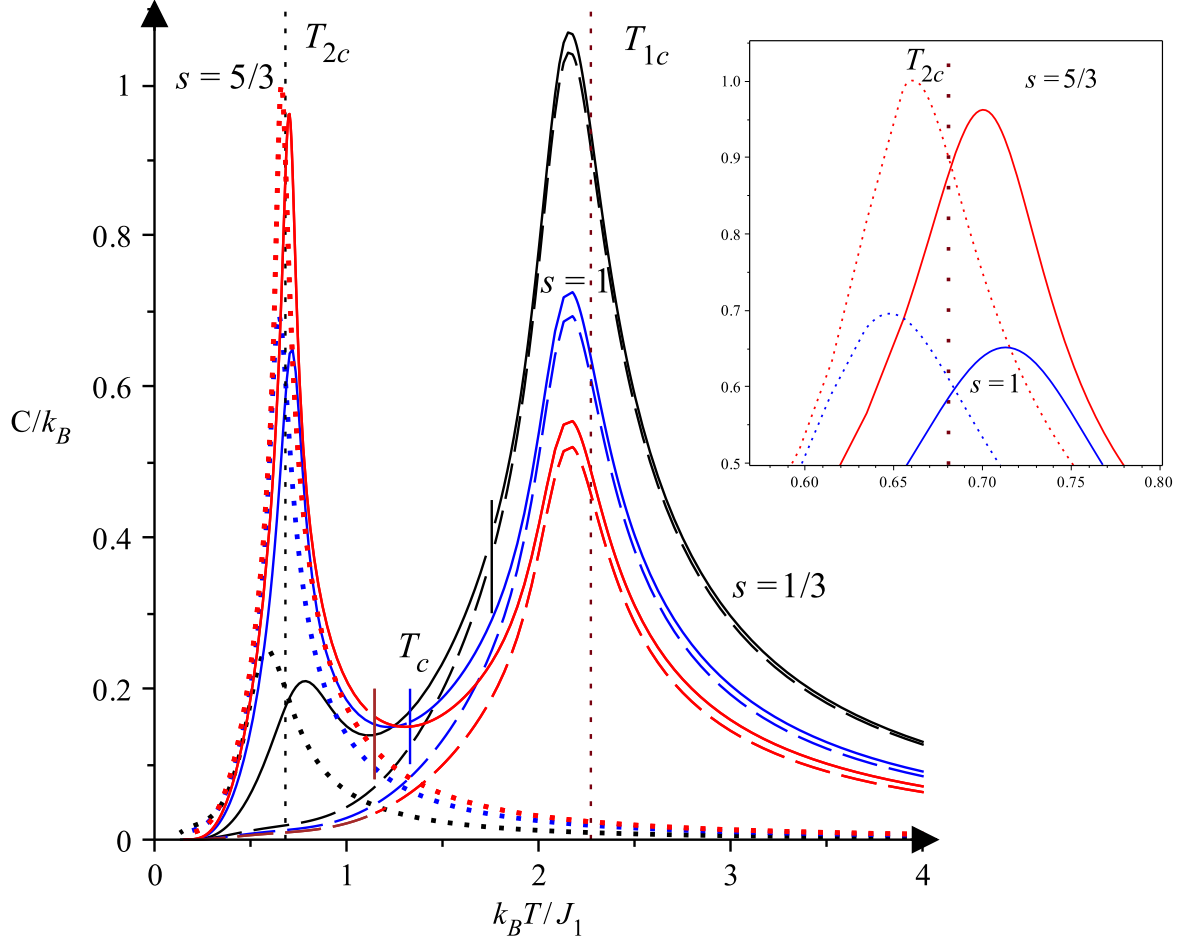


FIG. 4. Specific heat plots for relative strength $r = 0.3$ (as in Figs. 2(a) and 3) but with relative separations $s = 1/3, 1$ and $5/3$ when $m_1 = 18$. Again the decoupled $r = 0$ behavior is seen in the dashed plots while for the opposite limit, $r \rightarrow \infty$, the plots are dotted. The inset shows various coupled and uncoupled maxima near T_{2c} . The short vertical lines locate the bulk critical points, $T_c(r, s)$, which decrease as s increases.

perature T_c may be characterized by a correlation length $\xi(T)$ which diverges on approach to criticality as

$$\xi(T) \approx \xi_0/|t|^\nu \quad \text{with} \quad t = (T/T_c) - 1 \rightarrow 0, \quad (7)$$

where ν is a characteristic critical exponent while ξ_0 is a length of order the lattice spacing a , or molecular size, etc. For 2D Ising systems one has^{2,3,11,13} $\nu = 1$, whereas for superfluid helium in three bulk dimensions $\nu \simeq 0.67$ ¹. Then in a system limited in size by a finite length $L = \ell a$, the scaling hypothesis asserts, in general terms, that when ℓ and $\xi(T)$ are large enough, the rounding of critical point singularities is primarily controlled by the ratio $y = L/\xi(T)$.

Consequently, for the finite-size behavior of the specific heat per site, which diverges in bulk as $|t|^{-\alpha}$ where α is typically small (or even negative), the basic scaling hypothesis may be expressed as

$$C(\ell; T) \approx \ell^{\alpha/\nu} [Q(x) - Q_0]/\alpha, \quad (8)$$

where $Q(x)$ is the scaling function while the scaled temperature is

$$x = \ell^{1/\nu} t \propto y^{1/\nu} = [L/\xi(T)]^{1/\nu}, \quad (9)$$

and $Q_0 > 0$ is a constant parameter. The exponent α in the denominator in (8) allows for the limit $\alpha \rightarrow 0$, which yields, with $Q(0) \rightarrow Q_0$, a logarithmic singularity as is appropriate for 2D Ising systems. One may then take

$$C(\ell; T) \approx (Q_0/\nu) \ln \ell + Q(\ell^{1/\nu} t) \quad (10)$$

as the basic hypothesis where, for use below, we note that at criticality one has $C(\ell; T_c) \approx (Q_0/\nu) \ln \ell + Q(0)$. In fact, this hypothesis has been established explicitly for infinite Ising strips of width ℓ and $Q(x)$ has been explicitly determined¹⁶.

To apply these concepts to our layered Ising system, in the first case for the upper maxima near T_{1c} , we recall from Fig. 3 and Fig. 4 that leaving aside relatively small enhancements in magnitude, the total specific heat, $C(J_1, J_2; T)$, approaches rather well the limiting forms¹⁶ of a suitably normalized single strip of width m_1 . Accordingly, we subtract a contribution from *non-coupled* weaker Ising strips by defining

$$C_1(J_1, J_2; T) = (1 + s)[C(J_1, J_2; T) - C(0, J_2; T)], \quad (11)$$

where the normalization factor $(1 + s)$ is needed for the scaling plots now to be examined. Finally in accord with (10) and the subsequent remark we introduce the upper or stronger *net finite-size contribution*

$$\Delta C_1(J_1, J_2; T) = C_1(J_1, J_2; T) - C_1(J_1, J_2; T_{1c}), \quad (12)$$

in which the value at the *limiting* critical point, T_{1c} , has been subtracted. If we accept the identifications $\ell \Rightarrow m_1$ and $t \Rightarrow (T/T_{1c}) - 1$ and recall $\nu = 1$, we might expect $\Delta C_1(T)$ to obey scaling in terms of the variable

$$x_1 = m_1[(T/T_{1c}) - 1]. \quad (13)$$

This expectation is very well supported by the plots in Fig. 5 for $m_1 = 18$ and $s = n/3$ for $n = 1, 2, \dots, 5$: the “data collapse” is strikingly well realized.

Beyond this, however, explicit calculations⁹ show that, asymptotically, $\Delta C_1(T)$ is simply related to the limiting scaling function, $Q^\infty(x_1)$, for an infinite strip of coupling J_1 and width m_1 already known explicitly¹⁶. Specifically, allowing for normalization, yields

$$\Delta C_1(J_1, J_2; T) \approx (1 + s)[C(J_1, 0; T) - C(J_1, 0; T_{1c})] \approx Q^\infty(x_1) - Q^\infty(0). \quad (14)$$

Note that in this limit not only has the dependence on m_2 dropped out but also the dependence on J_2 . However, as regards the enhancement seen in Figs 2 to 4, we know that m_2 and J_2 do play a role. This will be studied further below.

Let us now shift attention to the behavior of the specific heat peaks of the alternating system, near the lower (or weaker) limiting critical point, T_{2c} . The rounded maxima are shown in detail in the insets of Figs. 3 and 4. Now we can follow the procedure that led to the definition (11). Thus we consider the normalized difference

$$C_2(J_1, J_2; T) = (1 + s^{-1})[C(J_1, J_2; T) - C(J_1, 0; T)]. \quad (15)$$

Then, following again the previous analysis, the *weaker net finite-size contribution* may be defined as in (12), by

$$\Delta C_2(J_1, J_2; T) = C_2(J_1, J_2; T) - C_2(J_1, J_2; T_{2c}). \quad (16)$$

It is natural to suppose that $\Delta C_2(T)$ might obey scaling in terms of the new variable

$$x_2 = m_2[(T/T_{2c}) - 1]. \quad (17)$$

This hypothesis is tested in Fig. 6 and, evidently, is remarkably successful, exhibiting excellent data collapse. But more remarkable yet is the evidence provided by the solid line plotted in Fig. 6. This derives directly from the limiting scaling function for an infinite strip of coupling J and finite width m^{16} but with the sign of the argument *reversed*. In other words, the previous asymptotic form (14) is now, as established in⁹ replaced by

$$\Delta C_2(J_1, J_2; T) \approx (1 + s^{-1})[C_2(0, J_2; \check{T}) - C_2(0, J_2; T_{2c})] \approx Q^\infty(-x_2) - Q^\infty(0), \quad (18)$$

where the modified temperature \check{T} is simply attained by reflecting about T_{2c} ; explicitly we have

$$\check{T}(T) = T_{2c} - (T - T_{2c}) = 2T_{2c} - T. \quad (19)$$

We may note, further, that in this limit the original dependence on both J_1 and m_1 has vanished; but, once more, there are clear residual effects associated

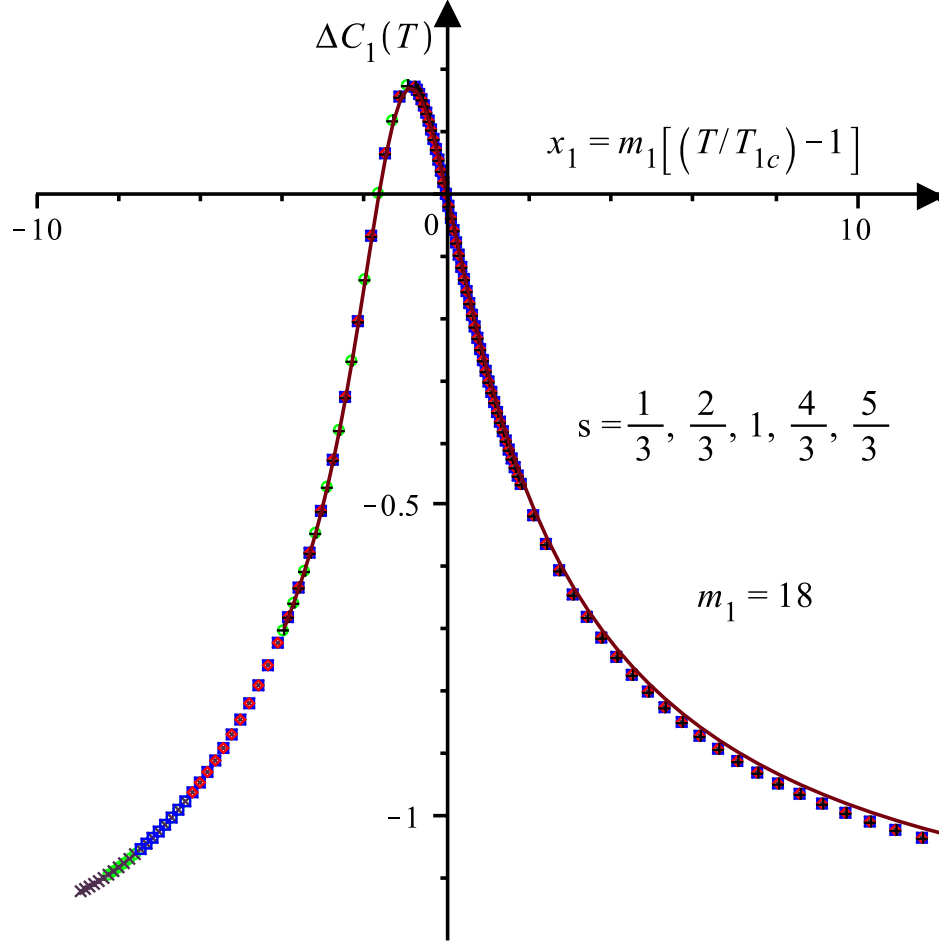


FIG. 5. Plot of the upper or stronger net finite-size contribution, namely, $\Delta C_1(J_1, J_2; T)$ as defined in the text for strong strips of width $m_1 = 18$ at various separations but fixed $r = 0.3$. The solid curve is the plot of the specific heat of an infinite strip of width $m_1 = 18$ and coupling J_1 when its value at the bulk critical temperature T_{1c} is subtracted¹⁶.

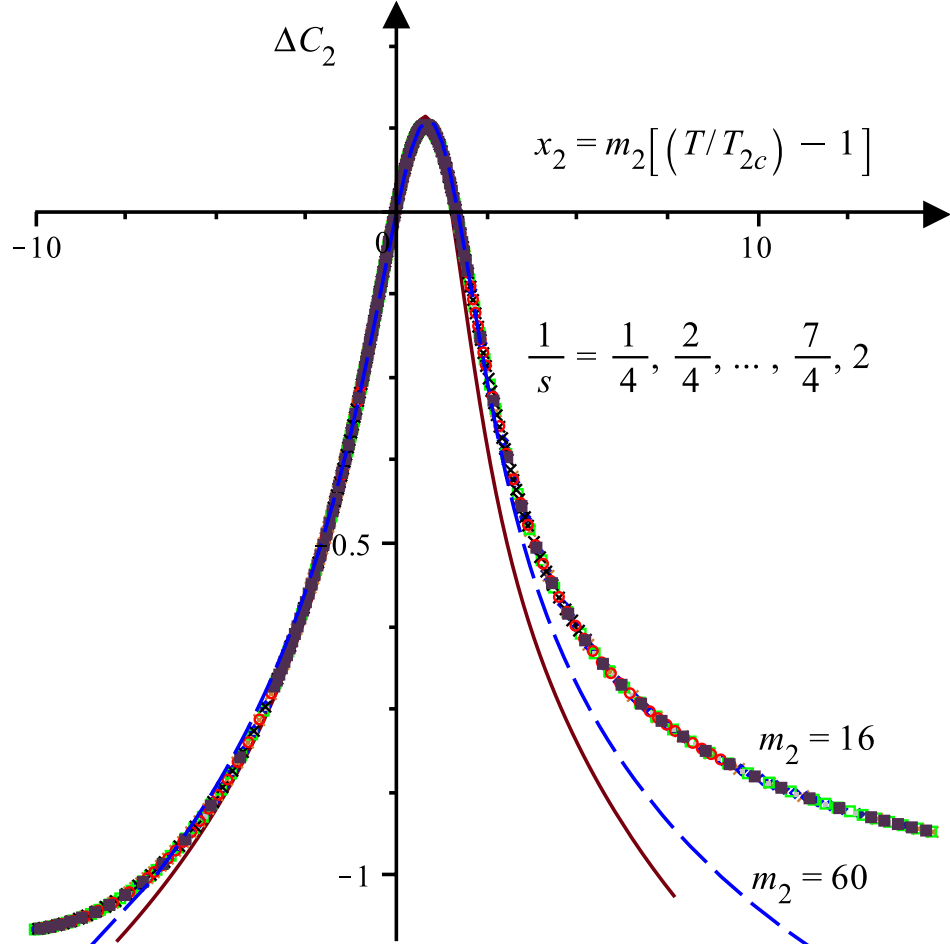


FIG. 6. Plots versus the scaling variable $x_2 = m_2[(T/T_{2c}) - 1]$ of the lower or weaker net finite-size contribution $\Delta C_2(J_1, J_2; T)$, as defined in relations (15)-(16), for strips of width $m_2 = 16$ and $r = 0.3$ for various relative separations. The solid curve represents the corresponding asymptotic form $Q^\infty(-x_2) - Q^\infty(0)$, for an infinite strip of finite width and coupling J_2 , with the temperature *reflected* about $T = T_{2c}$ ¹⁶. The dashed curve represents data for a wider strip with $m_2 = 60$.

with the proximity and interlayer couplings. To address these we may define an “enhancement” by subtracting from the total specific heat per site contributions deriving from the corresponding independent uncoupled strips. However, in doing this we must recognize — following Fig. 6 and the result (18) — that a reversed or reflected temperature variable is needed around T_{2c} . To this end we utilize the modified temperature variable, $\check{T}(T)$, via equation (19). Thus we define the net “enhancement” for fixed m_1 and m_2 by

$$\mathcal{E}(J_1, J_2; m_1, m_2; T) = C(J_1, J_2; T) - C(J_1, 0; T) - C(0, J_2; \check{T}(r)). \quad (20)$$

It worth remarking parenthetically that in adopting this definition of the enhancement we are, in particular, utilizing the theoretical results (18,19) proved for the alternating Ising strips⁹. In more general situations (such as confined superfluid helium) the last term in (20) should be replaced by an asymptotic term obtained by an initial data analysis of the behavior close to T_{2c} such as led to the original (finite m_2) form in Fig. 6.

In Fig. 7, we plot the enhancement for our alternating Ising strips as a function of $t = [(T/T_c) - 1]$ for $m_1 = 8$ and various separations s . One sees that the logarithmic divergence at $t = 0$ is barely visible for $s = 1$, and essentially disappears for $s > 1$. In addition, as expected, the magnitude of the enhancement decreases as s (or m_2) increases; but by what law?

To address this question we recall, first, that the leading correction to the asymptotic form of the specific heat of an infinite strip of finite width m must arise from the two non-vanishing *boundary free energy contributions*^{11,13,16,17} which yield a total specific heat term of relative order $1/m$. The effect of this are already evident in Fig. 6 where the primary contribution (solid curve) is, especially for $x_2 \geq 2$, more closely approached by the data for $m_2 = 60$ than that for $m_2 = 16$. It is clear that

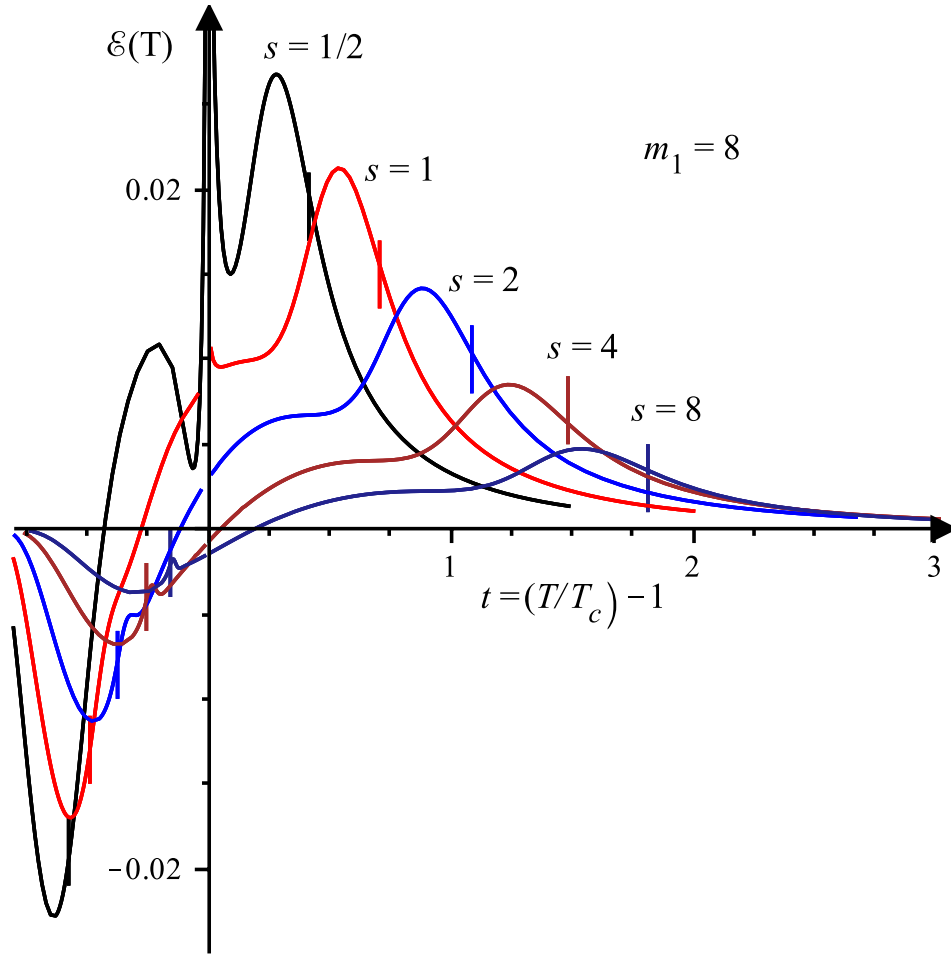


FIG. 7. Plots of the enhancement $\mathcal{E}(t)$ versus $t = (T/T_c) - 1$ for $m_1 = 8$, $r = 0.3$ and various relative separations s . The short vertical lines above $T_c(r, s)$, i.e., for $t > 0$ are the corresponding positions of T_{1c} , while below $T_c(r, s)$, they locate T_{2c} .

such corrections must arise also in the bulk alternating strip system from the regularly spaced modified boundary or *seams*. By the same token, boundaries of surface *effects* should play same role in the experiments on the specific heats of small helium boxes^{1,4,5,7,8} coupled via helium films.

Accordingly, Fig. 8 presents the enhancements $\mathcal{E}(t)$ versus $t \propto [T - T_c(r, s)]$, but

now multiplied by the factors $(m_1 + m_2)$, which clearly corresponds simply to the density of seams in the bulk. It is striking that the maxima (close to T_{1c}) and the minima (near T_{2c}) appear to rapidly approach constant values. This represents strong evidence that the enhancement $\mathcal{E}(J_1, J_2; m_1, m_2; T)$ is of order $1/(m_1 + m_2)$ as the relative separation, $s = m_2/m_1$, increases at fixed m_1 .

However, by comparing Figs. 8(a) and 8(b), it becomes clear that the behavior of the rescaled enhancement peaks that approach T_{1c} , when s increases, depend quite noticeably on m_1 , the width of the strong strips. Specifically, the enhancement peaks become both narrower, as indeed implied by Fig. 6, and taller as m_1 grows. Consequently, we will separately investigate the behavior of the enhancement close to T_{1c} , noting that some logarithmic dependence on m_1 might be present. Nevertheless, for $T < T_{1c}$ Fig. 8 suggests that the enhancement rescaled by $(m_1 + m_2)$ might approach a more or less constant shape when plotted against a suitable reduced intermediate temperature variable, say $t^\dagger(T; J_1, J_2; m_1, m_2)$.

Then, since the expected scaling behavior must switch in the region between T_{1c} and T_{2c} we consider a definition that may differ somewhat according to the sign of $t = [T/T_c(r, s) - 1]$. To that end, we may recall the known values of the bulk correlation lengths, $\xi_1(T)$ and $\xi_2(T)$, for the strong and weak strips at the bulk layered critical point $T_c(r, s)$, and note the ($T=T_c$) asymptotic identity (established in⁹) that states

$$\begin{aligned} c_1(J_1, J_2; m_1, m_2) &:= (1 + s^{-1})[(T_{1c}/T_c) - 1] \\ &\approx \xi_1^{-1}(T_c) + \xi_2^{-1}(T_c) := (1 + s)[1 - (T_{2c}/T_c)] = c_2. \end{aligned} \quad (21)$$

This suggests distinct but asymptotically equal rescaling factors for t above and below $T_c(r, s)$. Finally, it is convenient to arrange that $t^\dagger(T_{2c}) = 0$ and $t^\dagger(T_{1c}) = 1$: this yields the definition

$$t^\dagger(T) = t/c_1 + (1 + s)^{-1} \quad \text{for } t \geq 0,$$

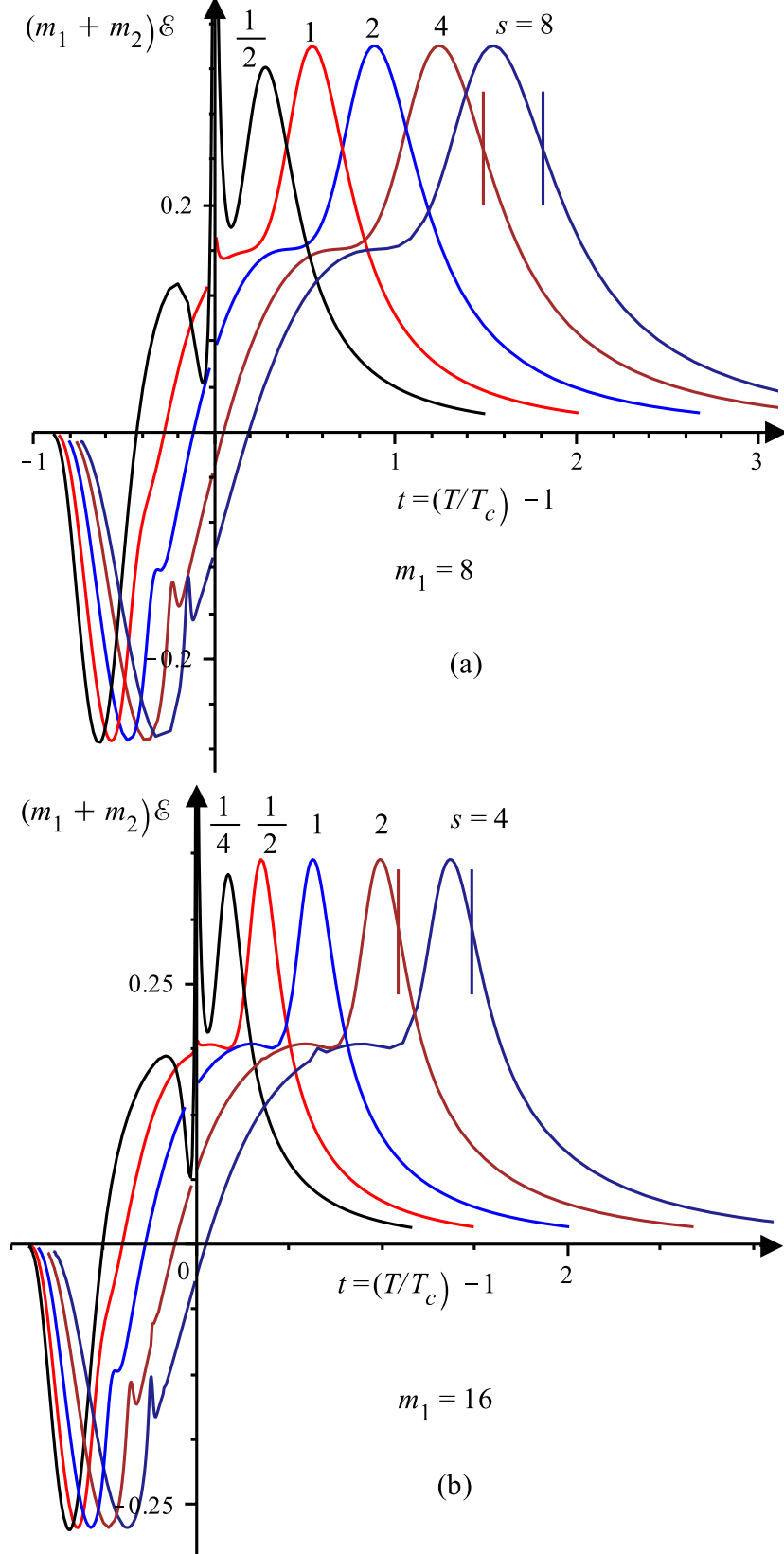


FIG. 8. The enhancement $\mathcal{E}(t)$: (a) for $m_1 = 8$ as in Fig. 7, and (b) for $m_1 = 16$, but multiplied by $(m_1 + m_2)$. The short vertical lines locate the corresponding upper limiting critical points, T_{1c} .

$$t/c_2 + (1 + s)^{-1} \quad \text{for } t \leq 0, \quad (22)$$

for which, as readily checked, the interval $t^\dagger(T_{1c}) - t^\dagger(T_{2c})$ is unity for all values of J_1 , J_2 , m_1 and m_2 .

Using this intermediate reduced temperature variable, Fig. 9 presents the rescaled enhancement in the range below $t^\dagger \simeq 1.5$ down to $t^\dagger \simeq -0.5$, where $\mathcal{E}(T)$ is negative and below which little remains to be seen. Note, however, that the rounded peaks close to $t^\dagger = 1$ have been omitted. While some peculiar rapidly varying features appear in the interval for $t^\dagger = 0$ to 0.1 associated with the limiting behavior of the subtracted third term in the enhancement definition (20), the overall set of data support the hypothesis of a universal limiting plot when $s \rightarrow \infty$ for large m_1 .

Finally, we investigate the enhancement in the vicinity of T_{1c} , recalling first, the subtracted and scaled total specific heat plots presented in Fig. 5. The maxima of the enhancement as m_1 runs from 8 to 64 are studied in Table I. Table I lists the values of $(m_1 + m_2)\mathcal{E}_{1c}(m_1)$ evaluated at T_{1c} and $(m_1 + m_2)\mathcal{E}_{max}(m_1)$ together with their ratio. Extrapolation of the ratio suggests a finite limit $\mathcal{E}_{max}/\mathcal{E}_{1c} \simeq 1.06$. This is consistent with a finite-size scaling expression for the asymptotic shape of the enhancement peaks. However, it is clear that the values of $(m_1 + m_2)\mathcal{E}_{1c}$ rise steadily with m_1 . As already hinted, in light of the leading asymptotic behavior relation (10) a logarithmic factor in the correction terms must be anticipated (although seemingly absent for $T \leq T_{2c}$ as evidenced by Figs. 8 and 9). In fact the slightly extrapolated fit

$$(m_1 + m_2)\mathcal{E}_{1c}(m_1) \simeq 0.0800 \ln(m_1/m_0), \quad m_0 = 0.36, \quad (23)$$

seems optimal as may be judged from the last column of Table I, which records the ratio $\mathcal{R}(m_1)$ of the two sides of this expression.

Last, to study the asymptotic shape of the enhancement peaks, note from Fig. 5 that the associated total specific heat peaks near T_{1c} are displaced by a known

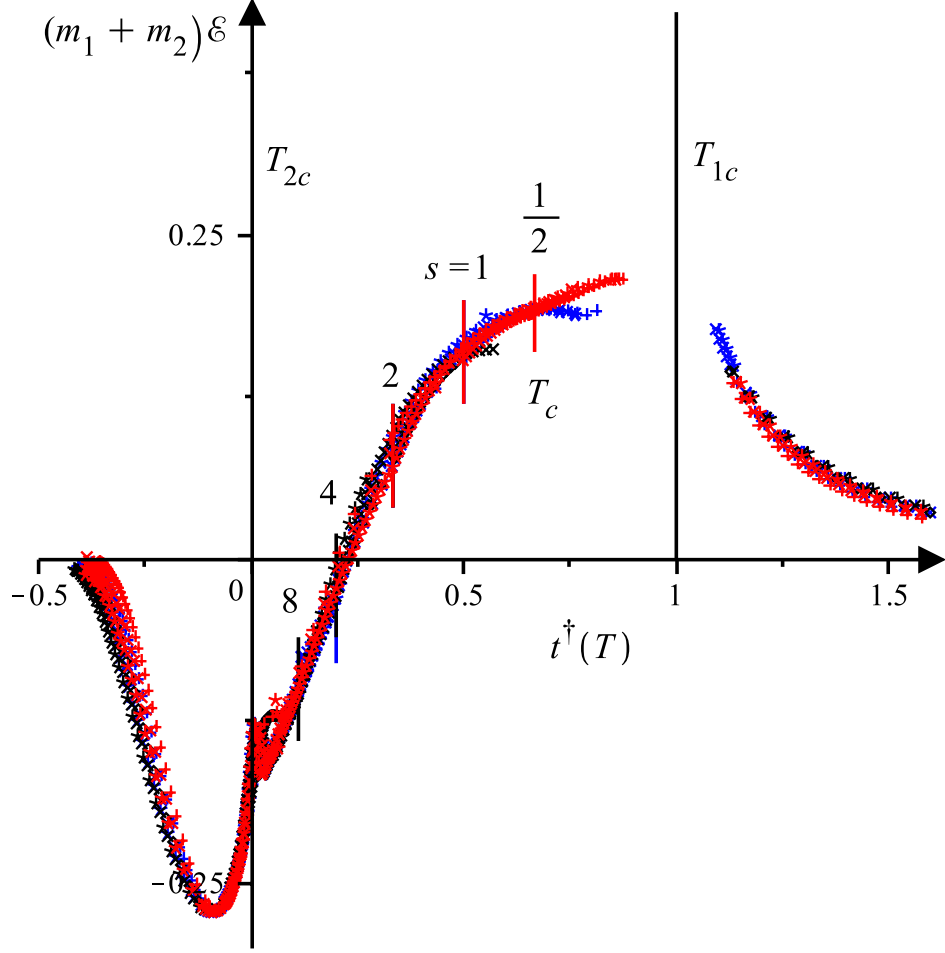


FIG. 9. Plots of the rescaled enhancement $(m_1 + m_2)\mathcal{E}(t)$ for $m_1 = 8, 16$ and 32 and separations $s = 1/2, 1, 2, 4, 8$ versus the reduced temperature variable, $t^\dagger(t)$, defined in the text. The color code is black for $m_1 = 8$, blue for $m_1 = 16$ and red for $m_1 = 32$.

scaled amount. Specifically, the scaled asymptotic maximum located at $x_1^{max} = x_1^0 = -0.7869^{16}$. The corresponding values of x_1 for the maxima of the enhancement as m_1 increases are listed in Table I together with the ratio $x^{max}(m_1)/x_1^0$. The data seem subject to numerical imprecision but inspection of the behavior of the ratio, say vs. $1/m_1$, we may reasonably conclude that the enhancement peaks, while of

somewhat different shape, with $x_1^{max}(m_1)/x_1^0 \rightarrow 0.6$, nonetheless, obey asymptotic finite-size scaling in terms of the strong bulk correlation length $\xi_1(T)$.

m_1	$(m_1 + m_2)\mathcal{E}_{1c}$	$(m_1 + m_2)\mathcal{E}_{max}$	$\mathcal{E}_{max}/\mathcal{E}_{1c}$	$\mathcal{R}(m_1)$	x_1^{max}	x_1^{max}/x_1^0
8	0.24884	0.34034	1.368	0.9989	-0.805	1.02
16	0.30386	0.36827	1.212	1.001	-0.917	1.17
24	0.33628	0.39241	1.167	1.001	-0.755	0.959
32	0.35936	0.41036	1.142	1.000	-0.662	0.842
40	0.37731	0.42505	1.127	1.000	-0.741	0.941
48	0.39197	0.43756	1.116	0.999(9)	-0.731	0.929
56	0.4044	0.4486	1.109	0.999(7)	-0.698	0.887
64	0.4152	0.4579	1.103	0.999(5)	-0.62	0.79

ACKNOWLEDGMENTS

The authors would like to thank F.M. Gasparini for discussions and correspondence. One of us (HA-Y) was supported in part by the National Science Foundation under grant No. PHY-07-58139.

* helenperk@yahoo.com

[†] xpectnil@umd.edu

- ¹ J. K. Perron, and F. M. Gasparini, M. O. Kimball, K. P. Mooney, M Diaz-Avila, *Finite-size Scaling of ^4He at the Superfluid Transition*, Rev. Mod. Phys. **80**, 1009–1059 (2008).
- ² M. E. Fisher, *Theory of Critical Point Singularities*, Sec.5, *Proc. 51st Enrico Fermi School, Varrenna, Italy: Critical Phenomena*, ed. M. S. Green, Academic Press, New York, 1–99 (1971).
- ³ M. N. Barber, *Finite Size Scaling in Phase Transitions and Critical Phenomena*, **8**, eds. C. D. Domb and J. L. Lebowitz, Academic Press, London, 145–266 (1983).
- ⁴ J. K. Perron, M. O. Kimball, K. P. Mooney, and F. M. Gasparini, *Lack of Correlation-length Scaling for an Array of Boxes*, J. Phys.: Conf. Ser. **50**, 032082–032084 (2009).
- ⁵ J. K. Perron, M. O. Kimball, K. P. Mooney, and F. M. Gasparini, *Coupling and Proximity Effects in the Superfluid Transition in ^4He Dots*, Nature Physics **6**, 499–502 (2010).
- ⁶ M. E. Fisher, *Superfluid Transitions: Proximity Eases Confinement*, Nature Physics **6**, 483–484 (2010). News & Views: Comment on⁵.
- ⁷ J. K. Perron, and F. M. Gasparini *Critical Point Coupling and Proximity Effects in ^4He at the Superfluid Transition*, Phys. Rev. Lett. **109**, 035302 (2012).
- ⁸ J. K. Perron, M. O. Kimball, K. P. Mooney and F. M. Gasparini *Critical Behavior of Coupled ^4He regions near the Superfluid Transition*, Phys. Rev. B. **87**, 094507 (2013).
- ⁹ H. Au-Yang, *Criticality in Alternating Layered Ising Models: II. Exact scaling theory*. Preprint arXiv:????.
- ¹⁰ B. Kaufman, *Crystal Statistics. II. Partition Function Evaluated by Spinor Analysis*, Phys. Rev. **76** 1232–1243 (1949).
- ¹¹ A. E. Ferdinand and M. E. Fisher, *Bounded and Inhomogeneous Ising Models I. Specific Heat Anomaly of a finite lattice*, Phys. Rev. **185** 832–846 (1969).
- ¹² M.E. Fisher, *Aspects of Equilibrium Critical Phenomena*, J. Phys. Soc. Japan (Suppl.) **26**, 87–93 (1969): see sec.7, Eqns (28)-(30).

- ¹³ B.M. McCoy and T.T. Wu, “The Two-Dimensional Ising Model,” Harvard Univ. Press, Cambridge, (1973).
- ¹⁴ H. Au-Yang and B.M. McCoy, *Theory of Layered Ising Model: Thermodynamics*, Phys. Rev. **B 10**, 886–891 (1974).
- ¹⁵ J.R. Hamm *Regularly Spaced Blocks of Impurities in the Ising Model: Critical Temperature and Specific Heat*, Phys. Rev. **B 15**, 5391–5411 (1977).
- ¹⁶ H. Au-Yang and M.E. Fisher, *Bounded and Inhomogeneous Ising Models II. Specific Heat Scaling Function for a finite Strip*, Phys. Rev. **B 11**, 3469–3486 (1975).
- ¹⁷ M.E. Fisher, and A. E. Ferdinand *Interfacial, Boundary, and Size Effects at Critical Points*, Phys. Rev. Lett. **B 19**, 169–172 (1967).